Multi-domain analysis of the microlensing survey data

Yogesh Joshi

Aryabhatta Research Institute of Observational Sciences (ARIES), India

Royal Observatory of Belgium, Brussels

12 October 2017

Outline of the Talk :

A brief introduction of gravitational lensing and microlensing

Nainital Microlensing Survey: Data acquisition and Reduction pipeline

Results of the Nainital Microlensing Survey

What is gravitational lensing

When a (foreground) massive object passes very close to line of sight of a (background) source, the gravitational field of foreground object forces the light of background source to deviate its path. Foreground object thus acts like a lens and phenomenon is called gravitational lensing.

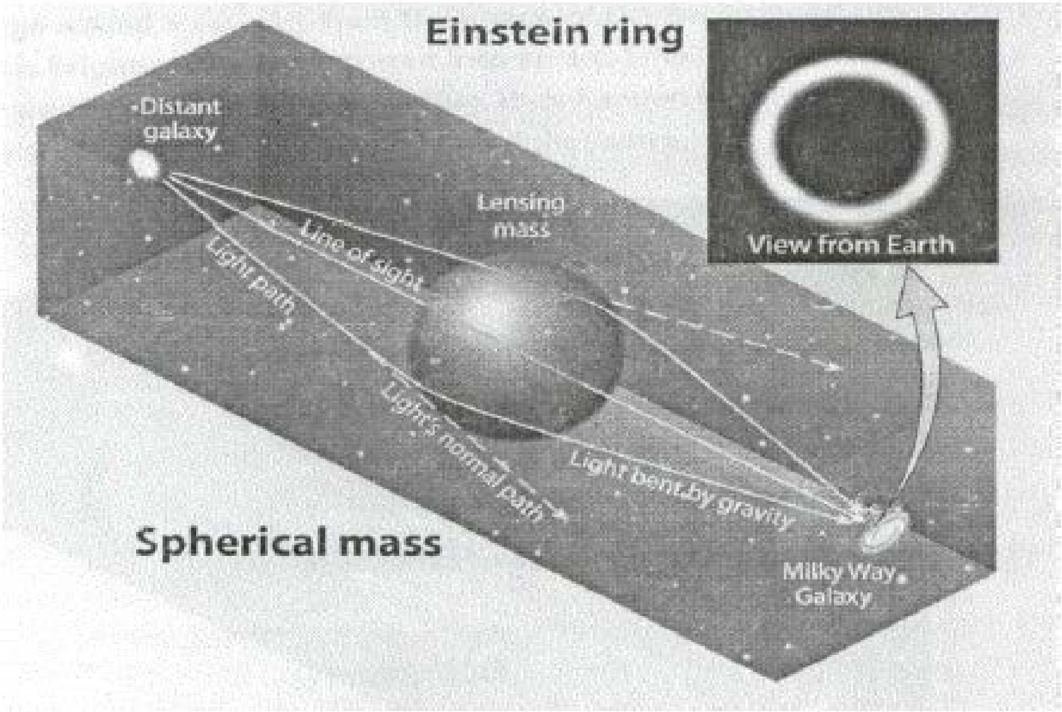

Gravitational microlensing

When stars in nearby region like Galactic bulge, Magellanic Clouds or M31 act as lenses, the deflection angle is a fraction of a milliarcsec. This is termed gravitational microlensing.

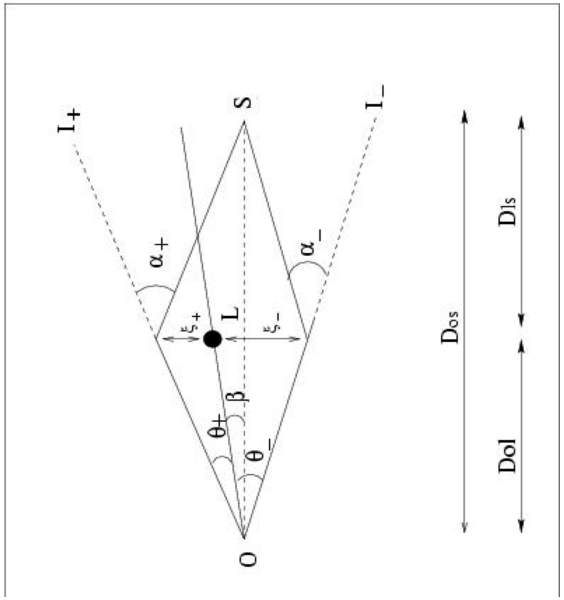

Microlensing event has following characteristics:

1. Shape of the light curve is symmetric around peak.
2. Achromatic phenomenon.
3. Does not repeat during 3-4 years observation

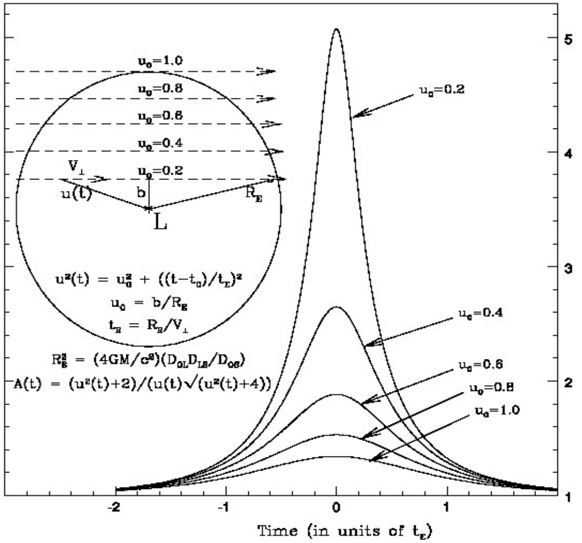

If we monitor a large number of resolved stars over a fairly long period of time then we may detect few of them.

Nainital Microlensing Survey

Motivation: Starting such survey in India

Indo-French collaborative program

Keeping the target in accordance with AGAPE collaboration

Difficult journey ahead with limited facilities!

Nainital Microlesning Survey: Data Aquisation

- Telescope: 104-cm Sampurnanand Telescope, Nainital
- CCD's used: 1K$\times$1K (FoV $\sim 6' \times 6'$) and 2K$\times$2K (FoV $\sim 13' \times 13'$)
- Central coordinates of the target field = $0^h 43^m 38^s$, δ = $+41^\circ 09'.1$
- Filters used: Cousin R (0.653 μ) and I (0.789 μ)
- Duration: 1998-1999 to 2001-2002 observing seasons (Oct.-Jan.)
- Total observed nights: 141 (133 in R & 116 in I)
- Exposure time per night: $\leq$40 min in R and $\leq$60 min in I
- Average seeing: $\sim$ 2.2 arcsec

Target field for Nainital Microlesning Survey

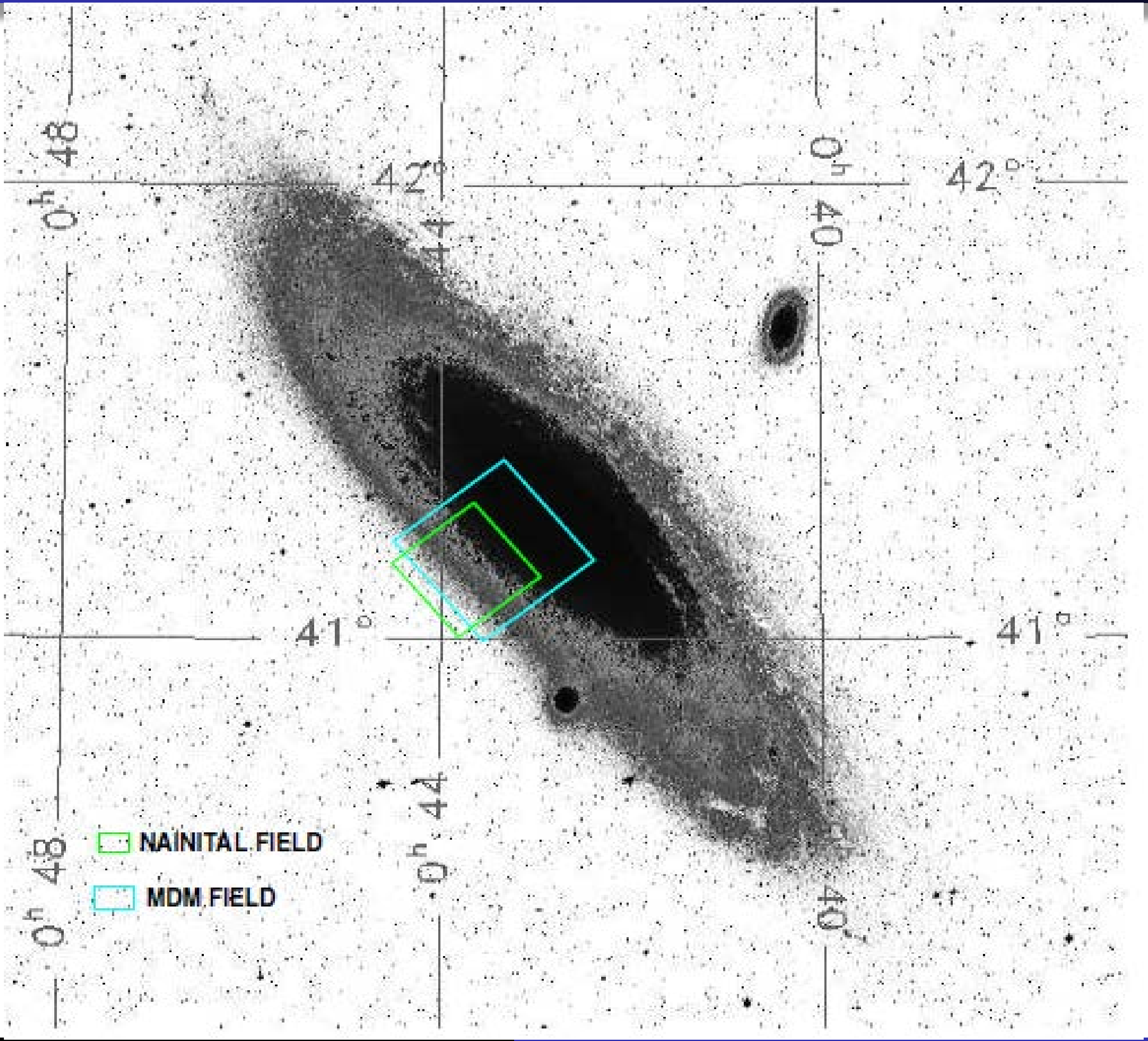

Problem with photometric analysis

- shape of the star
- seeing effect
- large sky background
- variable PSF
- surrounded in crowded region

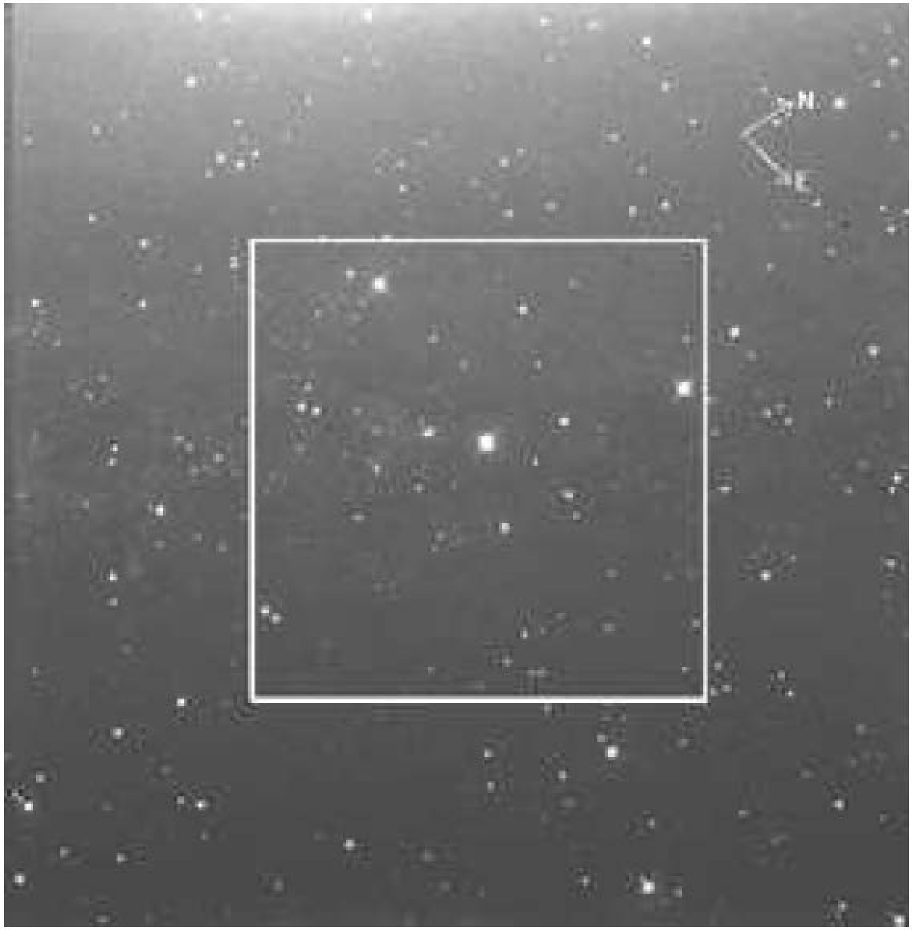

Figure 3.5: The $13' \times 13'$ target field in the direction of M31 reproduced from a 20 minute exposure in R band on 2k×2k CCD. The small rectangle shown in the image denotes $6' \times 6'$ field which was monitored using 1k×1k CCD. East and North directions are shown in the image.

Pixel Method and basic principle

Here we look for the flux variation of each pixel (or superpixel) of the CCD detector rather monitoring individual stars. In a CCD pixel, we get

$$F = F_* + F_{neighbours} + F_{sky}$$

Suppose the flux of target source F_* is amplified by a factor $A(t)$ at a particular time t, then the new flux of the pixel becomes

$$F' = A(t) \times F_* + F_{neighbours} + F_{sky}$$

Therefore the change in the flux of the pixel is

$$\Delta F = (A(t) - 1) \times F_*$$

Now if the target source shows a variation in flux with time, it will reflect in the ΔF and by plotting ΔF with the time, we can monitor the variation in the flux of the target source.

However, to detect any flux variation $\Delta F >> $ noise level

Alignment issues and Data analysis technique

To monitor the flux variations in any pixel, the images should be:

- **Geometrically aligned**: Each star should fall at the same pixel in all the frames.
- **Photometrically aligned**: All the frames should have the same sky background irrespective of atmospheric conditions.
- **Seeing Corrected**: Flux should be corrected for the seeing variation to reduce any unwanted fluctuation in the pixel light curve.

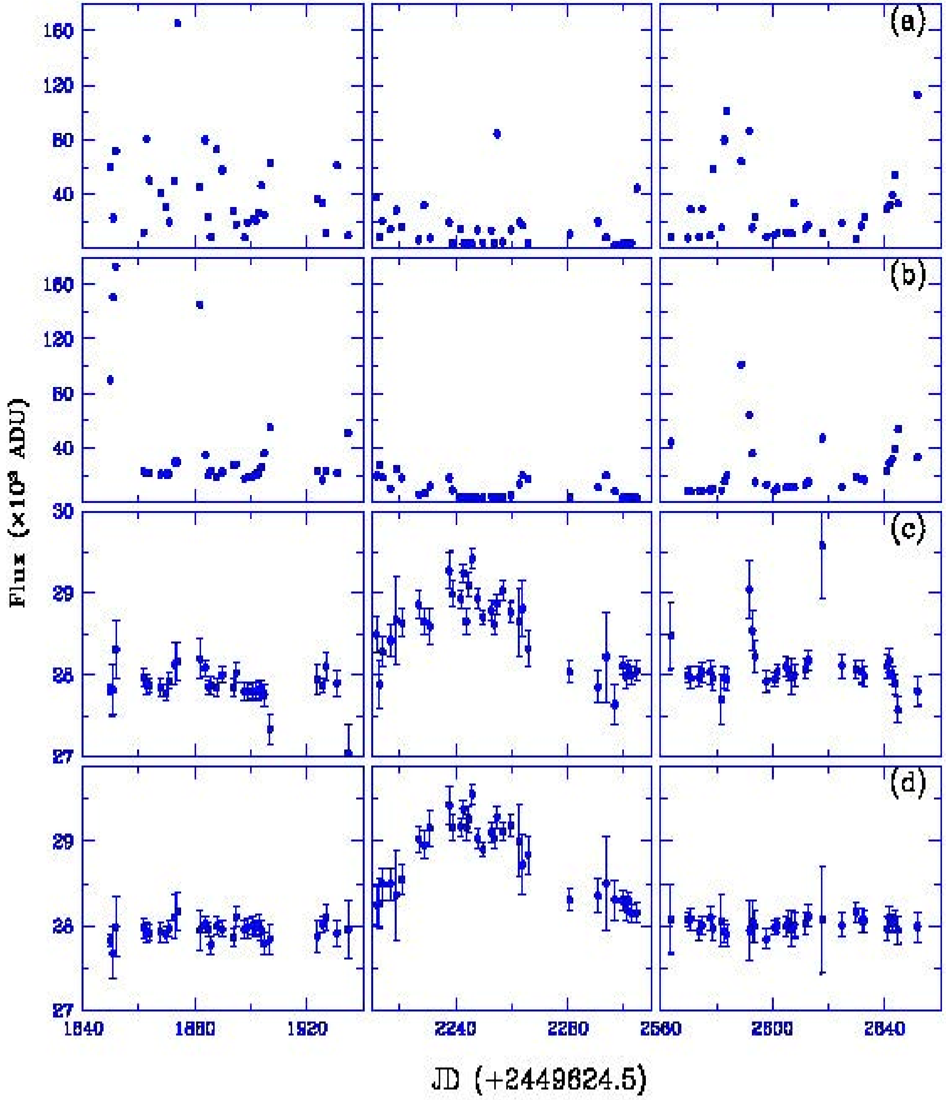

Discrimination of microlesning event from variable stars

Achromaticity:

Variable stars change in the temperature hence in colour. However, microlensing light curve is colour independent due to the gravitational origin of the lensing effect.

Symmetricity:

Most of variable stars show asymmetric flux variation with time. But, a microlensing light curve is normally symmetric in time around the maximum magnification.

Uniqueness:

There is a very rare possibility that a microlensing phenomenon occurs twice at a same place so one can reject all non-unique variations except when source or lens stars are well separated binary.

Hence, these properties of a light curve enable us to distinguish a microlensing event from the known types of intrinsic variability

Detection of first microlesning candidate event

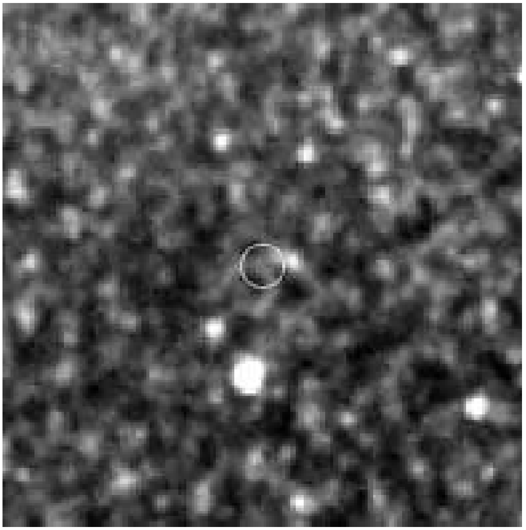

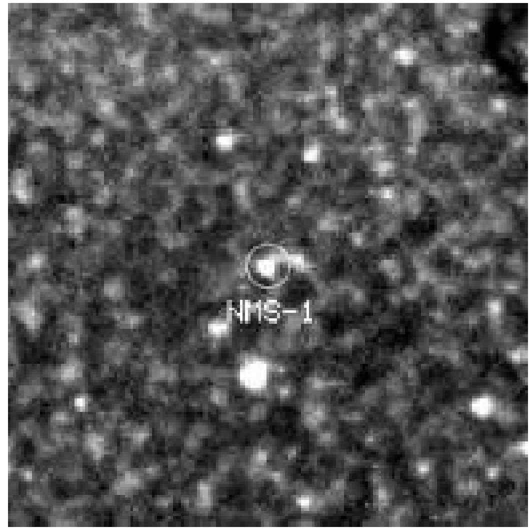

The positions of NMS-E1 shown by the circle. The left image shows no brightness at the pixel position while right image shows a amplified star at that position.

The light curves of NMS-E1 after subtracting the variable star contribution. A model microlensing fit is also drawn removing variable star contribution.

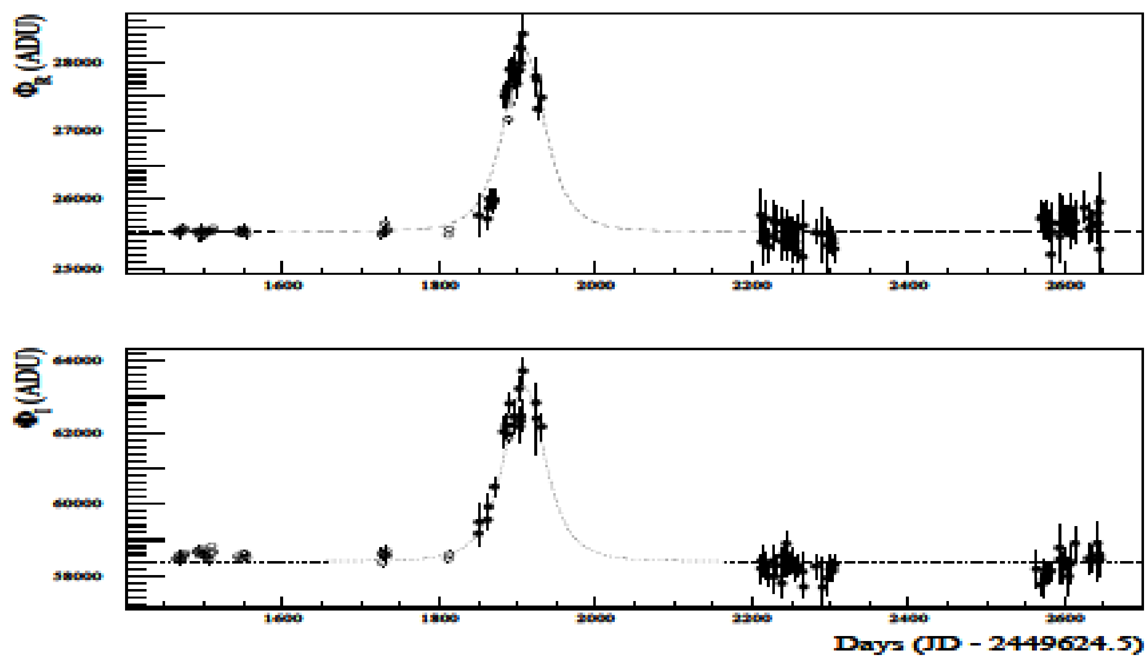

Physical interpretation of the event

$$R_{max} = 20.0 \pm 0.03, I_{max} = 18.8 \pm 0.03$$

Applying distance modulus of M31, we get

$$M_R = -5.12, M_I = -6.16, (R-I)_0 = 1.04$$

Then what it could be?

- either source is a M1-type main sequence star
- or source is a giant star

If it is a main sequence star $\Rightarrow A_{max} > 10^5$ which is very unlikely.

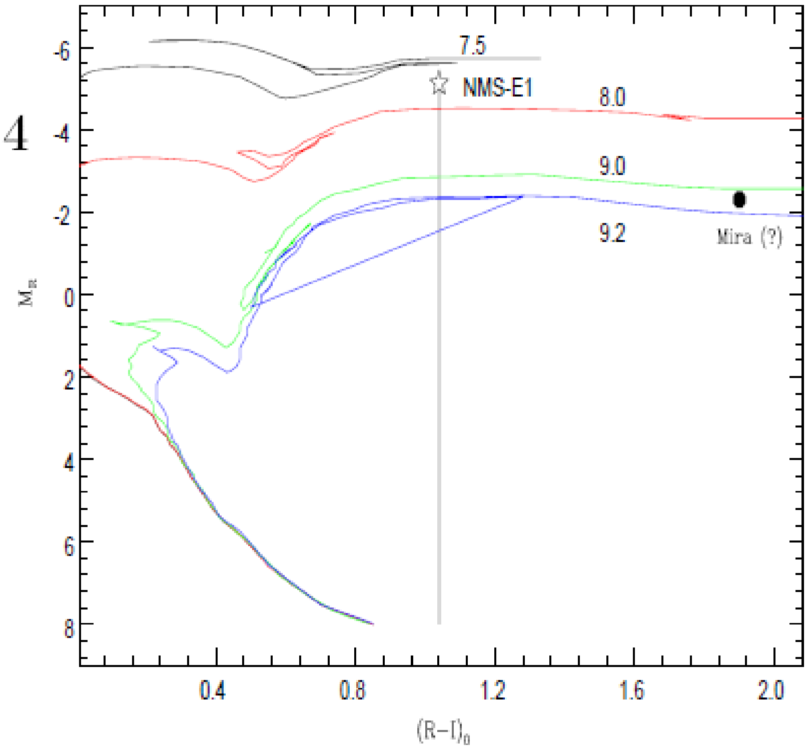

So, most probably it is a giant or sub-giant star for which $A_{max} > 6$

We conclude that:

- Candidate NMS-E1 could be due to halo lensing
- If it is say $\sim$ 22.5 mag then possible lens mass could be $M_{lens} \sim 0.5 M_\odot$

Variable stars as a bi-product of lensing survey

• The microlensing surveys have made it possible to discover and identify a large number of variable stars including Cepheid variables, RR Lyrae stars, long periodic variables (LPVs), etc.

The catalogues of variable stars compiled from such monitoring surveys are generally complete within limiting magnitude.

• One can determine precise pulsation period of the variables because of the long duration of survey and large number of observations.

• The large database allows the investigation of the metallicity effects in Cepheids, which have important implications on the cosmological distance ladder.

Detection of 26 Cepheids in the photometric survey

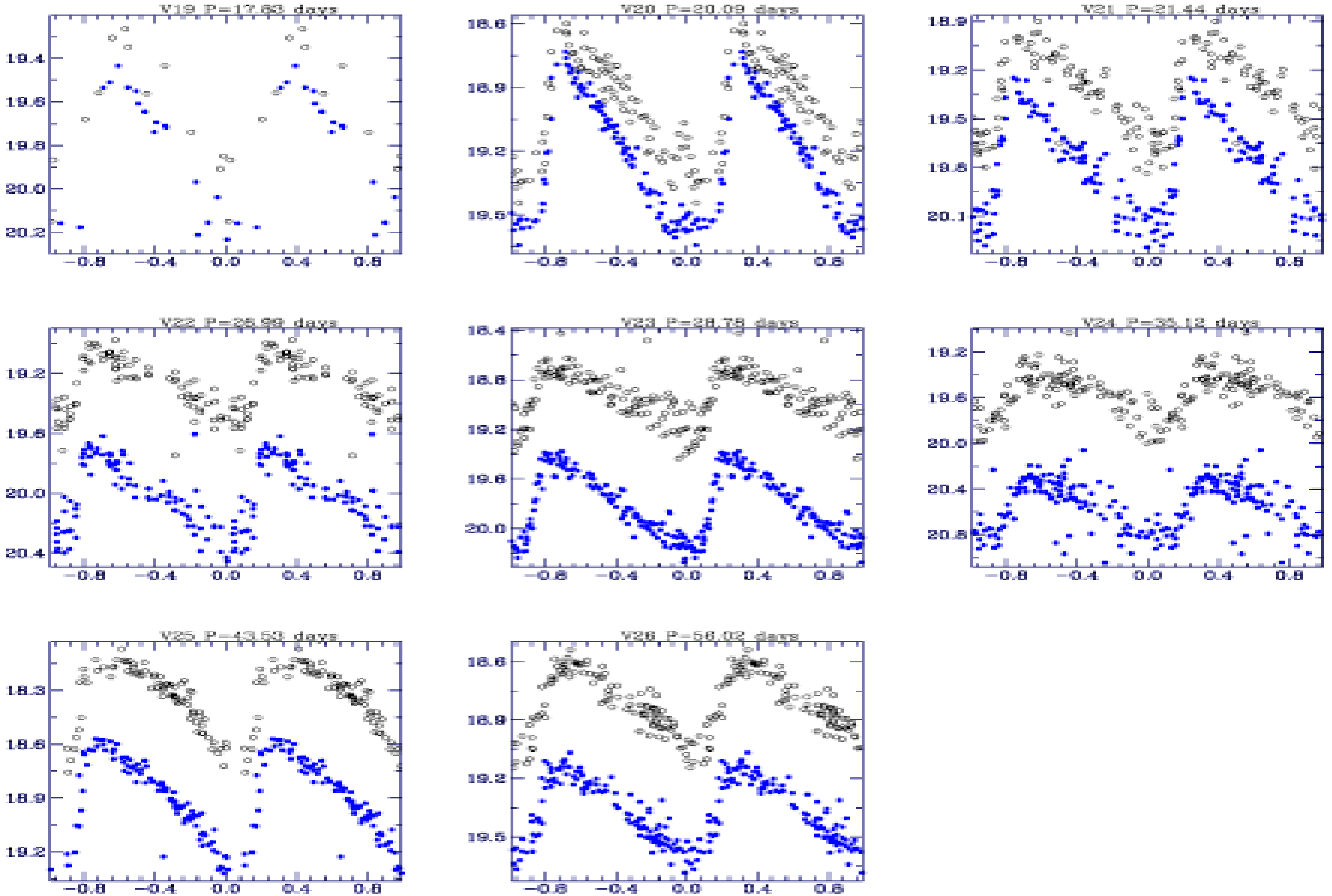

Table 4.2: A list of 26 Cepheids observed in the present study with their characteristic parameters. Star identification by KAL99, Tomaney & Crotts (1996), MAG97 and Berkhuijsen et al. (1988) are prefixed with K, TC, M and B respectively, in column 10. The periods of 13 Cepheids obtained in previous studies are given in the last column. The Cepheids which we discovered and classified are respectively marked as † and * in the first column.

Star ID	α (deg)	δ (deg)	$\overline{R}$ (mag)	$\overline{I}$ (mag)	Δ_R (mag)	Period (days)	Age (Myrs)	N	Other ID	Period (days)
V1	10.9321	41.1970	20.48	19.98	0.27	7.459±0.002	75	123	K V883	7.459
V2*	10.8469	41.1737	20.17	19.69	0.15	8.566±0.003	69	124	TC 170	—
V3*	10.8669	41.2320	20.61	20.28	0.22	8.836±0.004	68	120	TC 18	—
V4	10.9366	41.2503	20.28	19.54	0.11	9.160±0.008	67	86	K V1219	9.173
V5	10.9721	41.2128	20.56	20.04	0.19	9.790±0.005	64	92	K V2879	9.790
V6*	10.8770	41.0601	20.43	19.76	0.15	10.383±0.009	62	93	TC 76	—
V7*	10.8736	41.2367	20.42	20.27	0.28	10.500±0.004	61	123	TC 16	—
V8	10.7500	41.1426	19.89	19.55	0.17	11.17 ±0.01	59	95	M 65	25.0±5.0
V9*	10.8594	41.2004	20.21	19.60	0.26	13.773±0.006	52	126	TC 20	—
V10*	10.9290	41.1715	20.77	19.84	0.48	14.420±0.006	51	116	TC 85	—
V11	10.9255	41.2489	19.57	18.87	0.16	15.26 ±0.01	49	96	K V635	15.255
V12	10.9576	41.2227	20.84	20.08	0.32	15.46 ±0.01	49	89	K V2286	15.464
V13	10.8259	41.1386	19.82	19.46	0.40	15.76 ±0.01	48	94	M 68	14.0±2.8
V14*	10.9049	41.2419	19.93	19.58	0.22	15.90 ±0.01	48	121	TC 194	—
V15*	10.9115	41.2396	20.79	19.91	0.30	15.95 ±0.01	48	126	TC 196	—
V16	10.9775	41.2348	20.28	19.74	0.40	16.38 ±0.02	47	47	K V3198	16.345
V17*	10.9069	41.1868	20.12	19.60	0.39	16.60 ±0.01	47	124	B 4614	—
V18	10.9853	41.2176	19.47	19.09	0.21	17.73 ±0.01	45	91	K V3583	17.703
V19	10.9839	41.2374	19.83	19.60	0.32	17.83 ±0.03	45	18	K V3551	16.699
V20*	10.9526	41.1540	19.20	18.99	0.35	20.09 ±0.01	42	96	TC 207	—
V21	10.8379	41.1514	19.74	19.31	0.39	21.44 ±0.02	40	96	M 69	13.0±2.6
V22†	10.8272	41.1071	20.01	19.19	0.29	26.99 ±0.04	35	92	—	—
V23*	10.9059	41.2379	19.78	18.92	0.34	28.78 ±0.02	33	127	TC 30	—
V24†	10.9002	41.1823	20.55	19.57	0.23	35.12 ±0.05	30	121	—	—
V25	10.9293	41.2475	18.89	18.35	0.31	43.53 ±0.08	26	97	K V836	43.371
V26	10.9183	41.1856	19.36	18.82	0.22	56.02 ±0.08	22	124	K V164	56.116

P-L relation and distance of M31 galaxy

Using known LMC Cepheids, the standard Period-Luminosity relations are given as

$$M_R = -2.94(\pm 0.09) logP - 1.58(\pm 0.04)$$

$$M_I = -2.96(\pm 0.02) logP - 1.94(\pm 0.01)$$

We derived a P-L relation using 24 Cepheids as

$$R = -2.94 logP + 23.54(\pm 0.09)$$

$$I = -2.96 logP + 23.02(\pm 0.07)$$

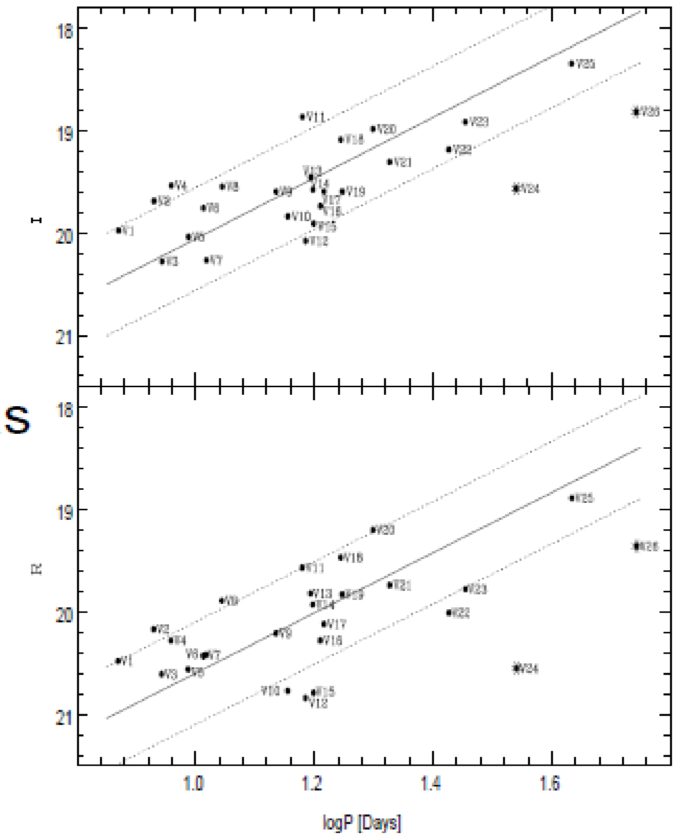

Thus the apparent distance modulus is

$$(m - M)_R = 25.12 \pm 0.09, \quad (m - M)_I = 24.96 \pm 0.07$$

Correcting for the extinction, it gives us a true distance modulus of

$$(m - M)_0 = 24.49 \pm 0.11 \quad \equiv \quad 790 \pm 45 \; kpc$$

Limitation of photometric technique in detection of faint Cepheids in M31

Most of the faint Cepheids towards M31 are 21-23 mag.

Using photometric technique they were not detected all the time

To draw a nice phase light curves, we need many detections at different phases

Hence we could detect only 26 Cepheids using photometric technique

However, we also used pixel method to identify faint low-period Cepheids in M31

Identification of faint Cepheids

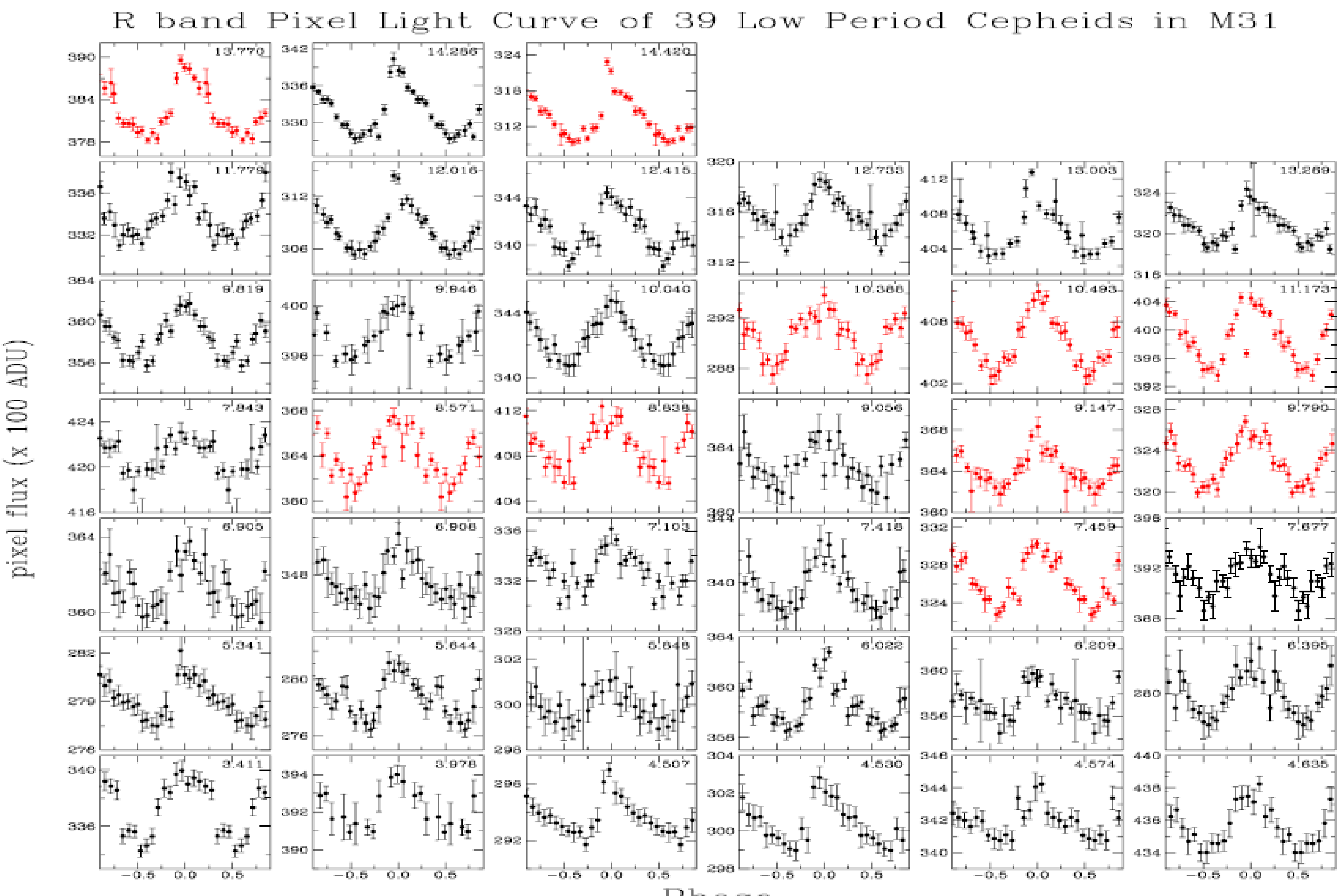

Identification of faint Cepheids

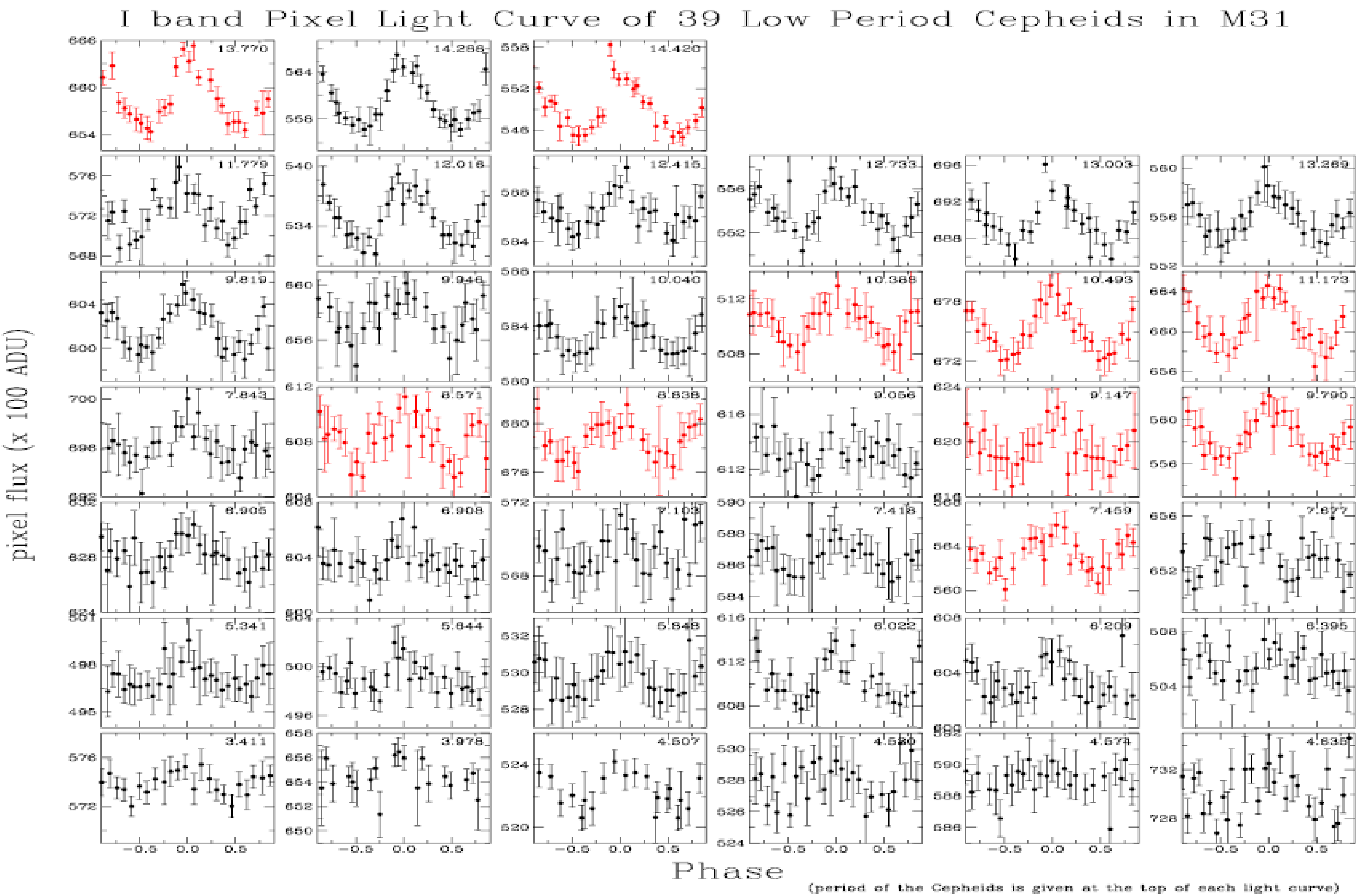

Detection of Novae in M31

A 2 arcmin wide subset of two different R band images taken on two different nights. The left image shows no star at the position marked by a circle while right image shows a star (nova NMS-1) of R = 17.2 mag at that position.

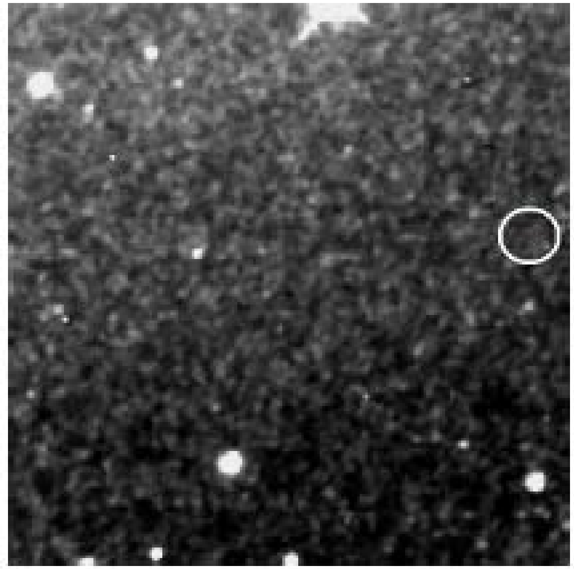

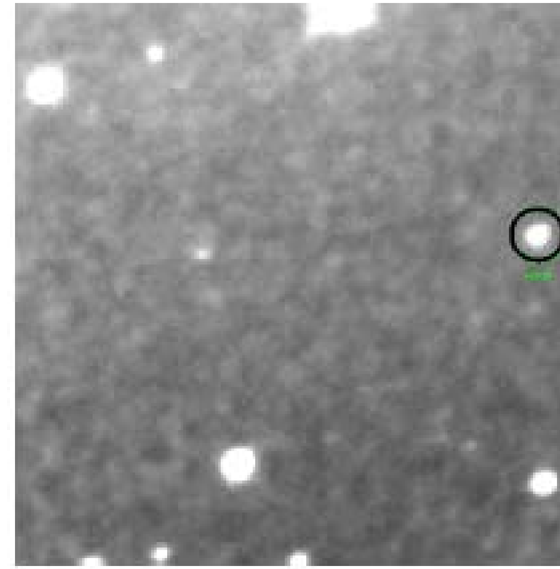

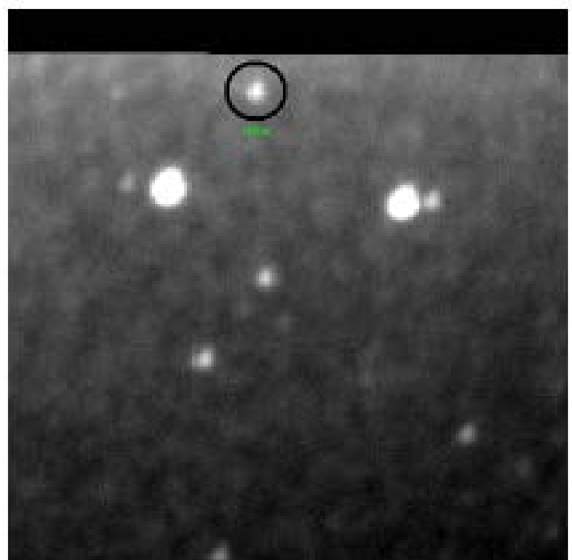

A 2 arcmin wide subset of two different images taken on two different nights. Right image shows a star (nova NMS-2) of R = 17.7 mag at that position.

Detection of Novae in M31

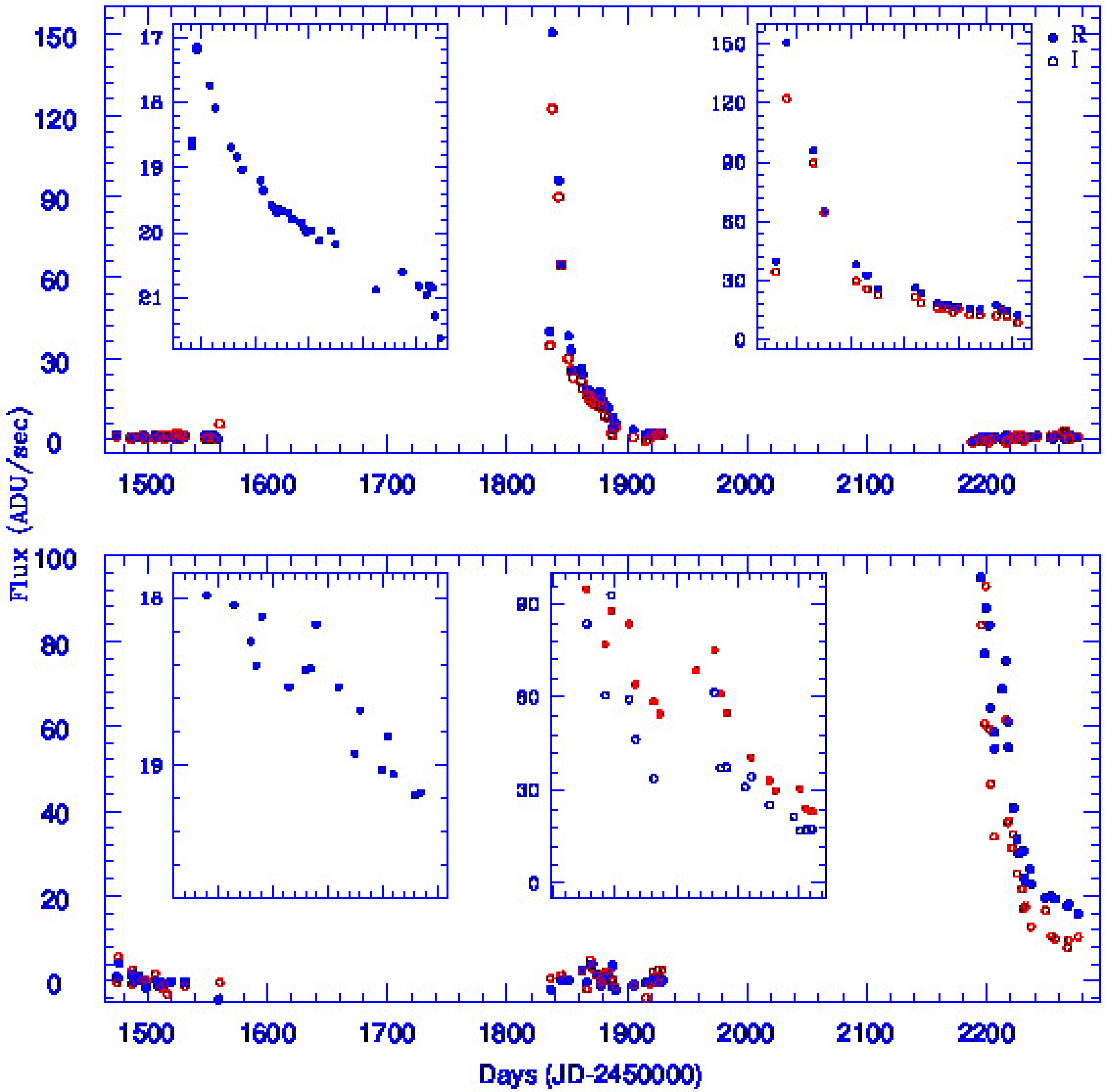

$t_{2,R} \sim 0.11 \text{ mag day}^{-1}$

$t_{2,I} \sim 0.11 \text{ mag day}^{-1}$

$$\frac{dM(R)}{dt} \sim 0.03 \pm 0.003 \text{ mag day}^{-1}$$

$$\frac{dM(I)}{dt} \sim 0.05 \pm 0.004 \text{ mag day}^{-1}$$

Detection of Eclipsing binary stars

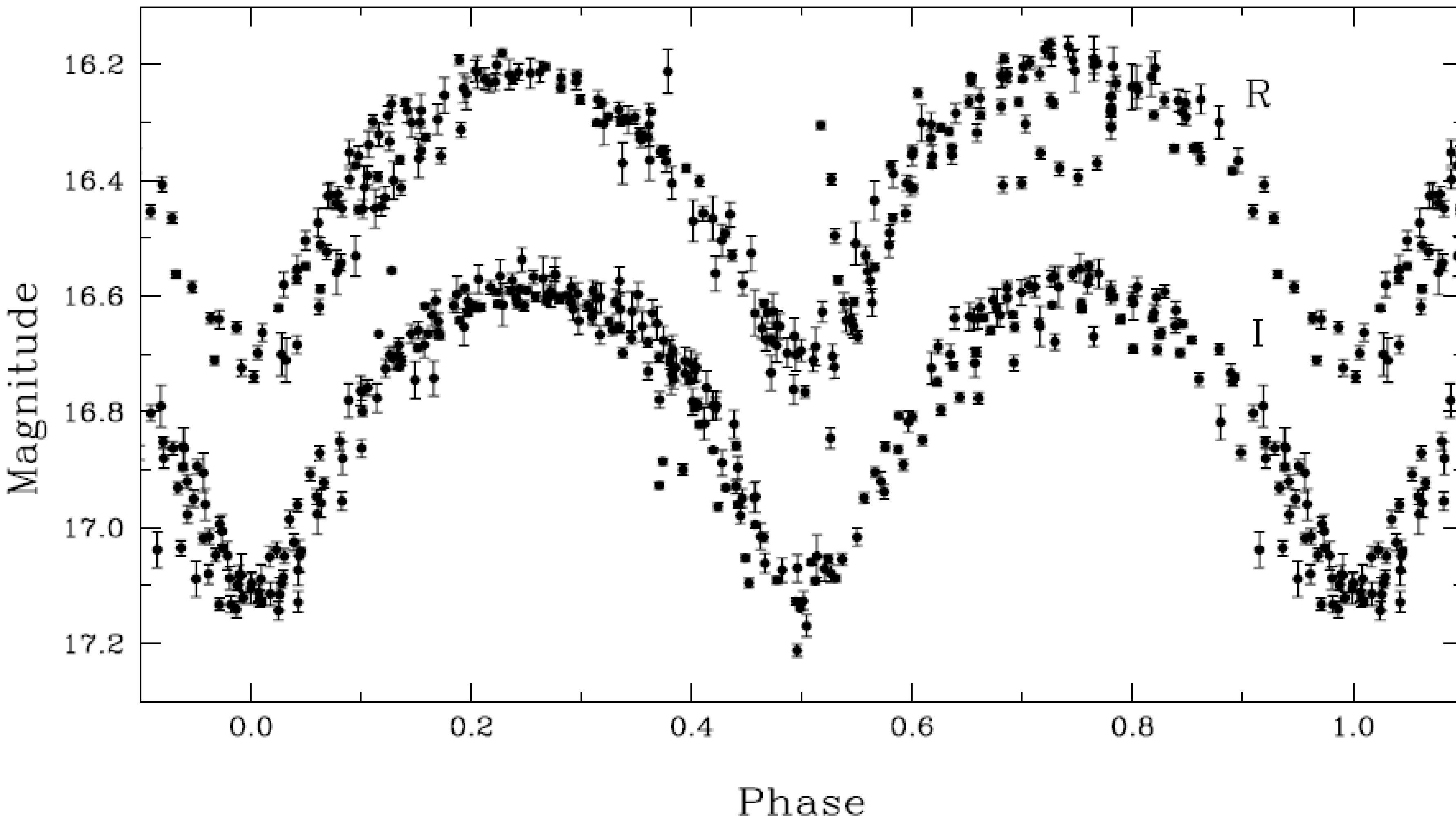

Fig. 3 Folded R_c and I_c bands phase light curves for the W UMa binary.

Analysis of Eclipsing binaries

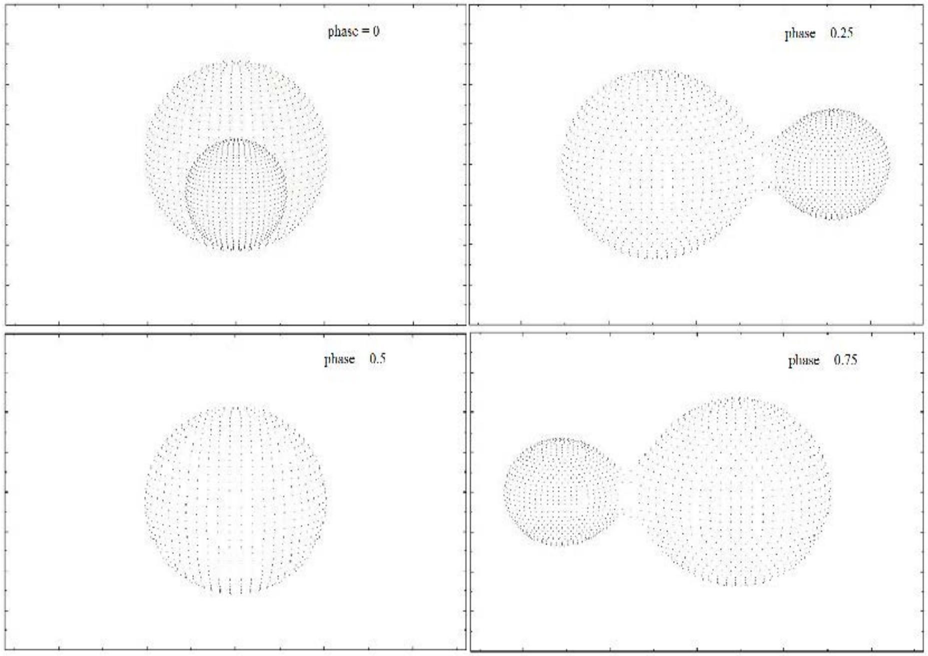

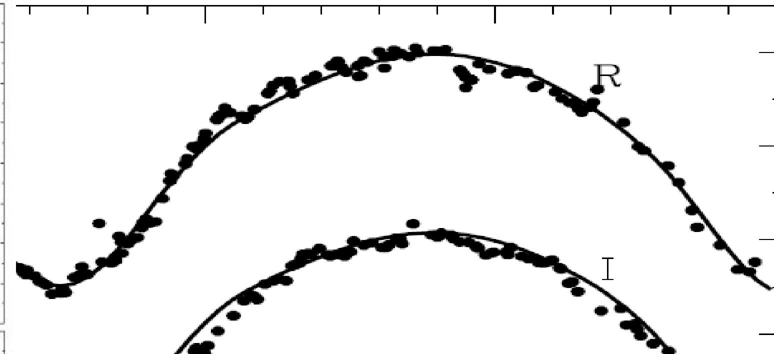

T_1 (K)	5724
T_2 (K)	5706 ± 55
Spectral Type	G3
q	0.28 ± 0.01
i_0	77.3 ± 0.4

arameters	R band	I band
M_1 $(M_\odot)$	1.19 ± 0.09	1.18 ± 0.09
M_2 $(M_\odot)$	0.33 ± 0.02	0.34 ± 0.03
R_1 $(R_\odot)$	1.02 ± 0.04	1.02 ± 0.04
R_2 $(R_\odot)$	0.58 ± 0.08	0.59 ± 0.02
L_1 $(L_\odot)$	0.69 ± 0.05	0.69 ± 0.05
L_2 $(L_\odot)$	0.24 ± 0.08	0.26 ± 0.03
M_{bol1}	5.17 ± 0.19	5.17 ± 0.19
M_{bol2}	6.31 ± 0.79	6.25 ± 0.28
ρ_1 (cgs)	1.61 ± 0.19	1.59 ± 0.19
ρ_2 (cgs)	2.50 ± 1.03	2.40 ± 0.25
$a(R_\odot)$	2.01 ± 0.05	
d (kpc)	2.64 ± 0.03	

Detection of exotic objects- Hubble Sandage variable

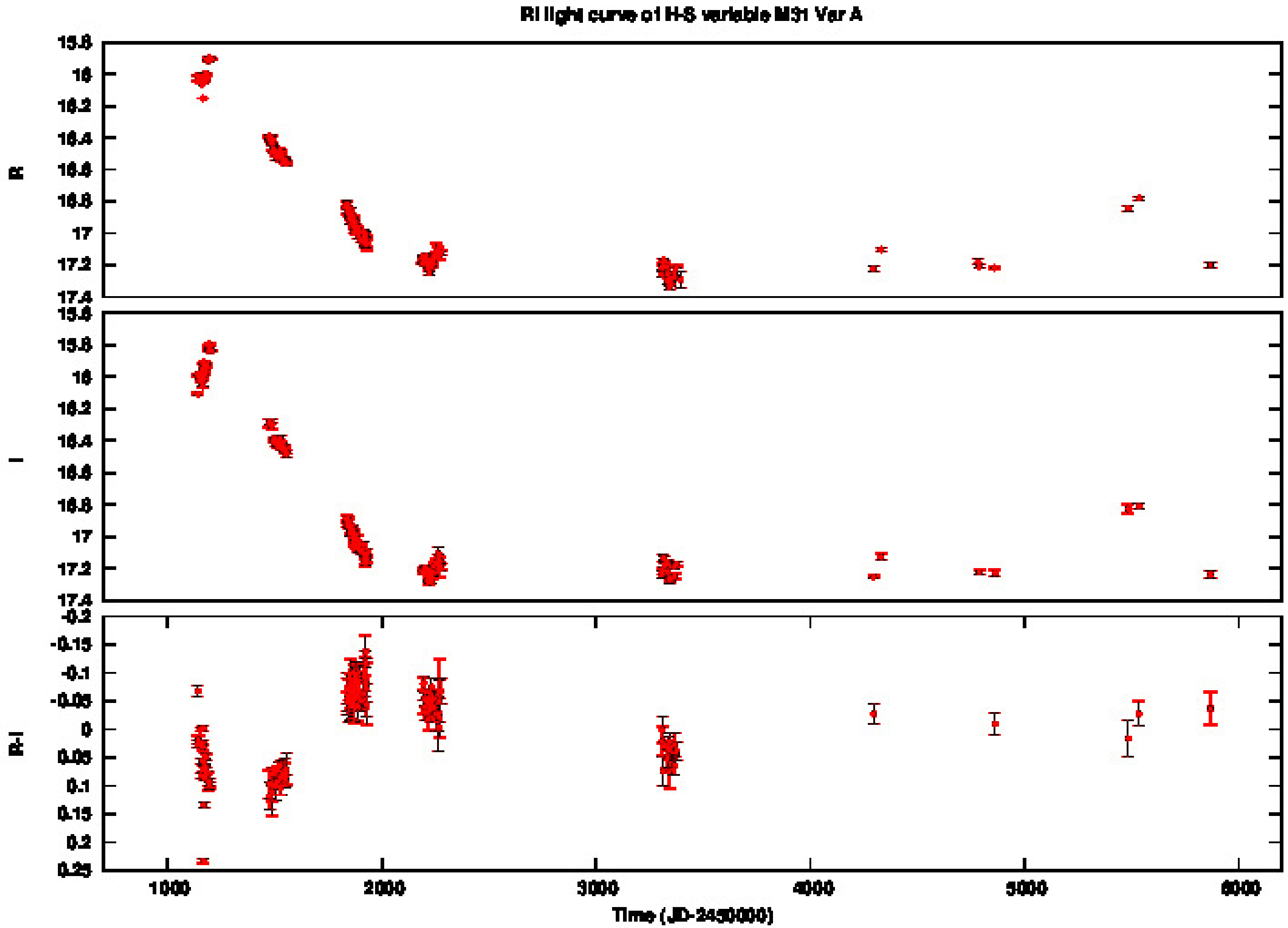

Summary of Nainital Microlesning Survey

1 microlensing candidate event was detected

26 bight Cepheids were detected using photometric technique

29 faint new Cepheids were detected using pixel technique

2 classical nova were detected

More than 330 variable stars including many eclipsing binaries were detected in the direction of M31 target field

Not all variable stars are analysed in detail.

Why this talk :

Research in Astron. Astrophys. **2017** Vol. **X** No. **XX**, 000–000
http://www.raa-journal.org *http://www.iop.org/journals/raa*

Research in Astronomy and Astrophysics

Long-term photometric study of a faint W UMa binary in the direction of M31

Y. C. Joshi[1] and Rukmini J.[2 ⋆]

[1] Aryabhatta Research Institute of Observational Sciences, Manora Peak, Nainital, India - 263002
[2] Center for Advanced Study in Astronomy, Osmania University, India

Received 15 June 2017; accepted 31 July 2017

Future survey with 4-m ILMT

Observatory

Aryabhatta Research Institute of Observational Sciences (ARIES)

Thanks

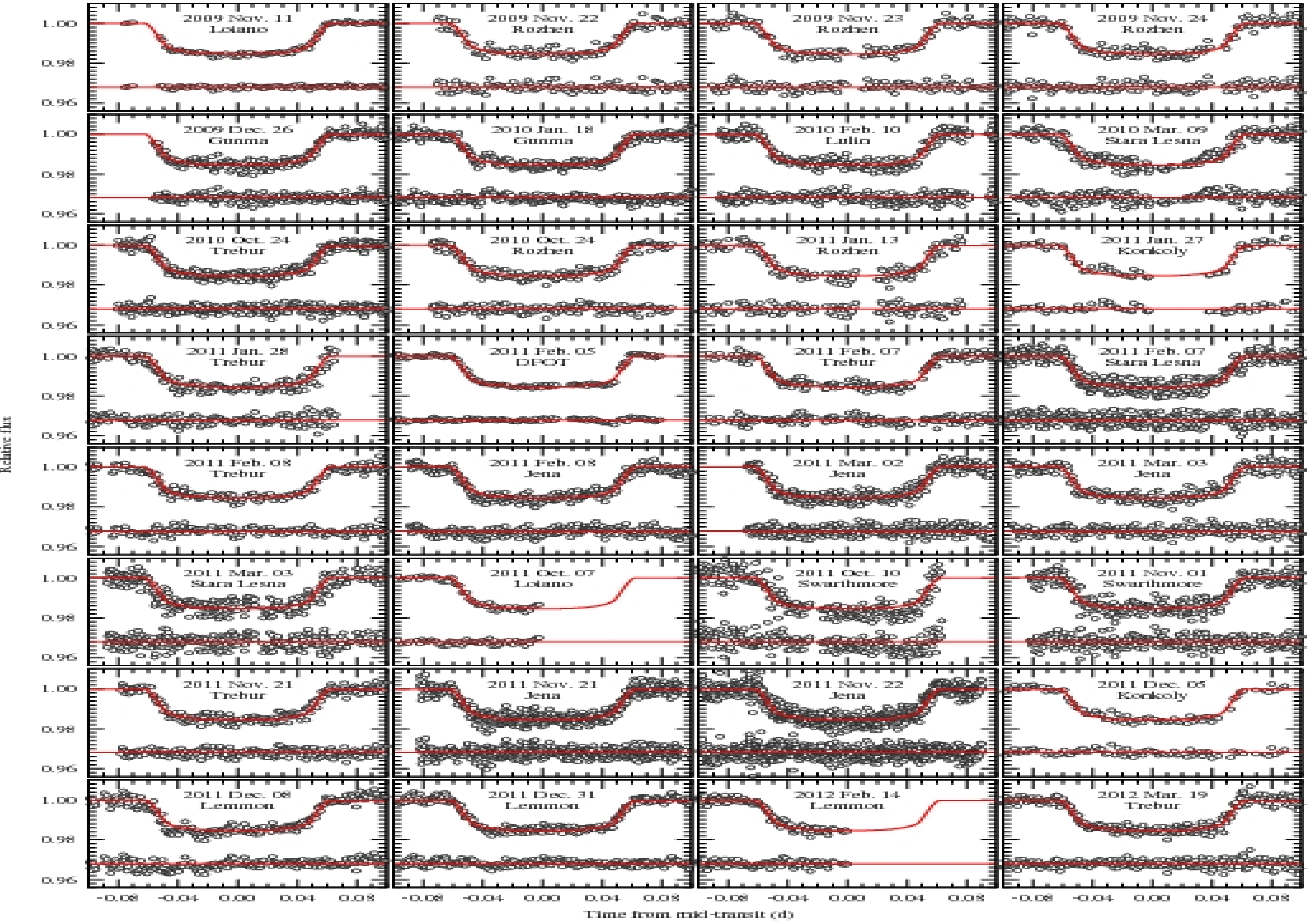

- Maciewski et al., including **Joshi, Y.C.**, 2013, A&A, 551, 108

Exciting time for Astronomy in India :

Participation in Mega Projects:
TMT, LIGO, SKA

Space missions:
ASTROSAT, ADITYA

New Telescopes:
3.6m DOT, 4-m ILMT, 2-m NLST

Under planning:
8 to 10 m NLOT

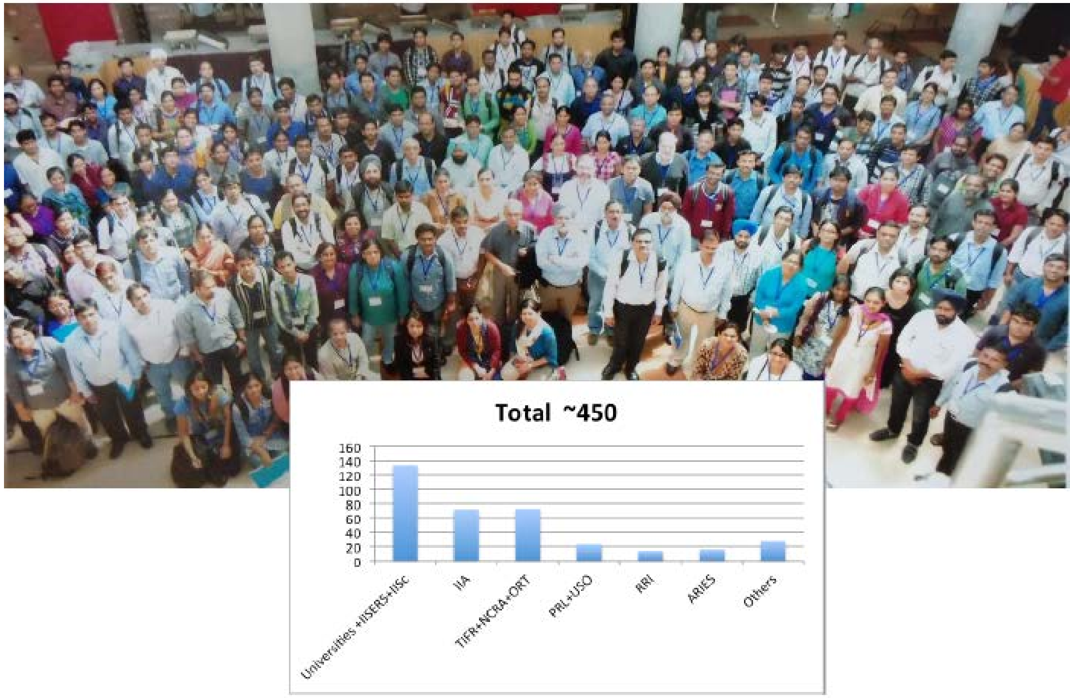

Human Resource

Locations of Indian Optical Facilities

IAO, Hanle

(Latitude : 32° 46´ N, Longitude : 78° 58´ E))

Devasthal, Nainital

(Latitude: 29° 22´ N; Longitude: 79° 41´ E)

VBO, Kavalor

Latitude: 12° 34´ N; Longitude: 78° 50´ E)

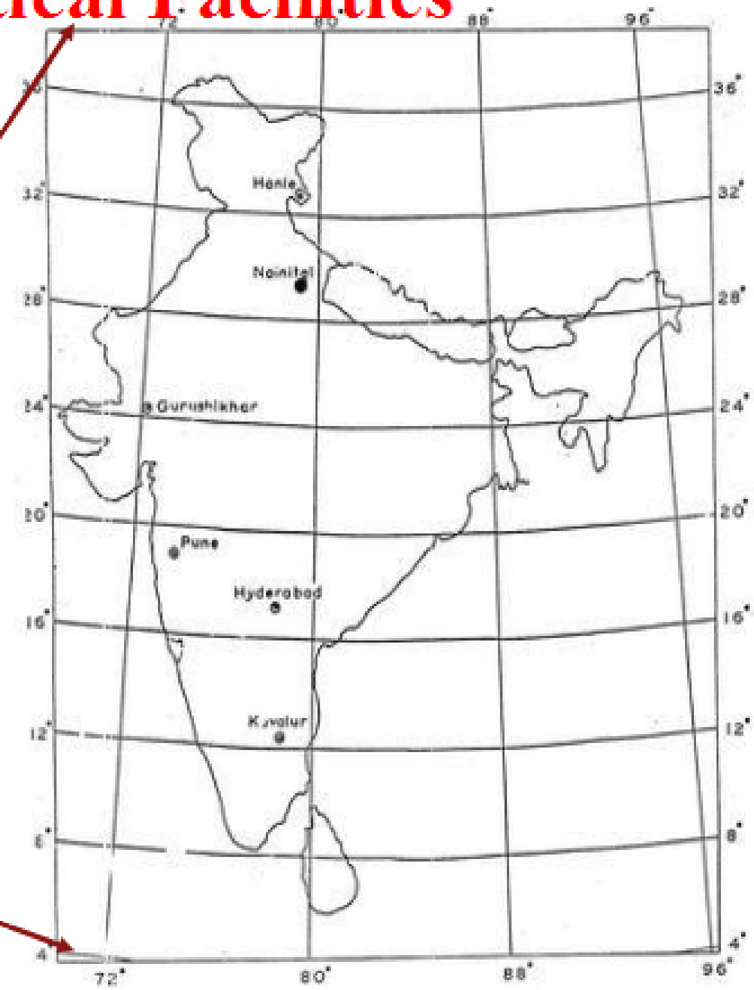

Longitudinal importance for time-critical and multi-site observations- India can fill the gap between Australian sky and the sky of Canary Island